

Impact of the spread-spectrum technique on the higher-order harmonics and radiated emissions of a synchronous buck converter

Original

Impact of the spread-spectrum technique on the higher-order harmonics and radiated emissions of a synchronous buck converter / Blečić, Raul; Bacmaga, Josip; Barić, Adrijan; Pareschi, Fabio; Rovatti, Riccardo; Setti, Gianluca. - STAMPA. - (2018), pp. 13-16. (Intervento presentato al convegno 2018 New Generation of CAS, NGCAS 2018 tenutosi a Valletta (Malta) nel 20-23 November 2018) [10.1109/NGCAS.2018.8572290].

Availability:

This version is available at: 11583/2728432 since: 2024-05-07T10:05:47Z

Publisher:

Institute of Electrical and Electronics Engineers Inc.

Published

DOI:10.1109/NGCAS.2018.8572290

Terms of use:

This article is made available under terms and conditions as specified in the corresponding bibliographic description in the repository

Publisher copyright

IEEE postprint/Author's Accepted Manuscript

©2018 IEEE. Personal use of this material is permitted. Permission from IEEE must be obtained for all other uses, in any current or future media, including reprinting/republishing this material for advertising or promotional purposes, creating new collecting works, for resale or lists, or reuse of any copyrighted component of this work in other works.

(Article begins on next page)

Impact of the Spread-Spectrum Technique on the Higher-Order Harmonics and Radiated Emissions of a Synchronous Buck Converter

Raul Blecic^{*}, Fabio Pareschi^{†‡}, Josip Bacmaga^{*}, Riccardo Rovatti^{§‡}, Gianluca Setti^{¶‡}, Adrijan Baric^{*}

^{*} University of Zagreb Faculty of Electrical Engineering and Computing, Unska 3, 10000 Zagreb, Croatia

[†] Engineering Department in Ferrara (ENDIF), University of Ferrara, 44100 Ferrara, Italy

[‡] Advanced Research Center on Electronic Systems (ARCES), University of Bologna, 40125 Bologna, Italy

[§] Department of Electrical, Electronic, and Information Engineering, University of Bologna, 40136 Bologna, Italy

[¶] Department of Electronics and Telecommunications, Politecnico di Torino, 10129 Torino, Italy

Tel: +385 (0)1 6129547, fax: +385 (0)1 6129653, e-mail: raul.blecic@fer.hr

Abstract—Switched-mode power converters generate electromagnetic emissions which may violate the limits specified in the regulations. Spread-spectrum is an effective technique for reducing the electromagnetic interference of switching devices. The reduction of the magnitude of the first harmonic by the spread-spectrum technique is mainly in focus in the literature. In this paper, the impact on the higher-order harmonics and on the radiated emissions is analyzed. A non-regulated synchronous buck converter is used as a device under test. The radiated emissions of the converter are calculated from the measurements performed by a transverse electromagnetic cell and a hybrid coupler. The measurements are performed for different values of the parameters of the spread-spectrum technique and a reduction of up to 5.7 dB is obtained.

Index Terms—electromagnetic compatibility, electromagnetic interference, power conversion, switched-mode power supply, transverse electromagnetic cell.

I. INTRODUCTION

Switched-mode power converters are sources of electromagnetic interference (EMI) which is a result of the switching operation and fast current changes (di/dt) and voltage changes (dv/dt) [1], [2]. The levels of the generated EMI may violate the limits specified in the regulations [3].

Spread-spectrum (SS) has been employed recently as an effective technique for reducing the EMI of switching devices [4]–[9]. All these papers use the SS to reduce in particular the magnitude of the EMI related to the first harmonic. This may be a limitation since the latter may not be the only spectral component violating the limits. For example, the maximum value of the radiated emissions of synchronous buck converters typically occurs in the frequency range from 50 to 300 MHz [10], although the switching frequency (i.e. the frequency of the first harmonic) is typically not larger than a few MHz.

In this paper, the impact of the SS technique on the higher-order harmonics and on the radiated emissions of a non-regulated synchronous buck converter is analyzed. The SS is applied to the control signal of the converter. The radiated emissions of the converter are calculated from the equivalent model of dipole moments, which are extracted from

the measurements performed by a transverse electromagnetic (TEM) cell and a hybrid coupler [11], [12]. The measurements are performed for different parameters of the SS technique.

Section II describes the principle of operation of the SS technique and its impact on the higher-order harmonics. Section III presents the impact of applying the SS to the radiated emissions of a synchronous buck converter. Section IV concludes the paper.

II. SPREAD-SPECTRUM TECHNIQUES

A. Principle of Operation

The SS techniques aim at spreading the energy of a narrowband signal by introducing new spectral components in the frequency spectrum. Since the SS techniques conserve total signal energy, their use is beneficial from the EM compatibility point-of-view since the magnitudes of the spectral components of the spread signal are smaller than those of the original one.

Among several possible SS techniques, the frequency modulation (FM) of a converter control signal (assumed to be a clock signal with the frequency f_{sw}) is considered in this paper and it is illustrated in Fig. 1. The parameters regulating the FM are the frequency f_m of the modulation signal, the frequency deviation Δf and modulation function $f(f_m)$. The frequency of the modulated control signal is given by:

$$f_{sw,FM} = f_{sw} + \Delta f \cdot f(f_m). \quad (1)$$

The impact of the SS technique on the EMI spectrum is determined by all three parameters of the FM. Most of the energy of each harmonic of the original signal is spread into the Carson's bandwidth which is proportional to Δf [13]. The modulation function defines the shape of the spectrum, while f_m defines, for a periodic modulation law, the separation of the spectral components. Increasing Δf or decreasing f_m introduces more spectral components within the Carson's bandwidth, thus reducing the average magnitude of these components. The modulation index m combines the two parameters as:

$$m = \Delta f / f_m. \quad (2)$$

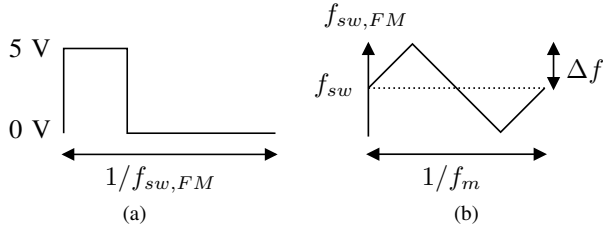


Fig. 1. Illustration of the FM: (a) one period of the converter control signal and (b) the frequency of the converter control signal as a function of the parameters of the FM (the triangular modulation function $f(f_m)$ is shown).

B. Impact of the Spread-Spectrum Technique on Higher-Order Harmonics

The frequency modulation of the converter control signal produces the same result as if applying the FM with different modulation parameters to each harmonic. More specifically, all harmonics are modulated by the same modulation frequency f_m , while the frequency deviation of the n -th harmonic is n times larger than Δf of the fundamental frequency. Let the equivalent frequency deviation Δf_n be defined as the frequency deviation of the n -th harmonic, calculated as:

$$\Delta f_n = n \cdot \Delta f. \quad (3)$$

The equivalent modulation index, i.e. the modulation index seen by the n -th harmonic, can be calculated as:

$$m_n = \frac{\Delta f_n}{f_m} = \frac{n \cdot \Delta f}{f_m} = n \cdot m. \quad (4)$$

The choice of Δf is typically a trade-off. High values maximize the impact of the SS technique. However, the upper value of Δf is always limited by the impact of the SS technique on the other characteristics of the switching device which can be tolerated for a specific application, such as the efficiency and the ripple of the output voltage in the case of synchronous buck converters.

Furthermore, increasing Δf leads to the overlap of the bands where the energy of higher-order harmonics is spread, with a possible reduction in the spread spectrum effectiveness. This occurs because the equivalent frequency deviation Δf_n increases linearly with the harmonic index, while the separation of two adjacent harmonics is fixed and equal to f_{sw} . Referring to the generic n -th harmonic, the overlap may occur both in the upper and lower frequency bands. The overlap of the spreading bandwidth around the n -th harmonic and around some lower n_1 -th harmonic (and, consequently, of the bandwidth of all harmonics in between) occurs if the sum of the equivalent frequency deviations is larger than the distance between the two original harmonics, i.e.

$$n \cdot \Delta f + n_1 \cdot \Delta f \geq (n - n_1) \cdot f_{sw}. \quad (5)$$

Equivalently, the overlap of the spreading bandwidth of the n -th, some higher n_2 -th harmonic and of all harmonics in between occurs if:

$$n \cdot \Delta f + n_2 \cdot \Delta f \geq (n_2 - n) \cdot f_{sw}. \quad (6)$$

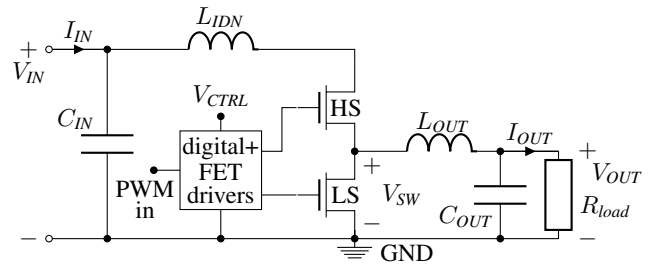


Fig. 2. Simplified schematic of a synchronous buck converter.

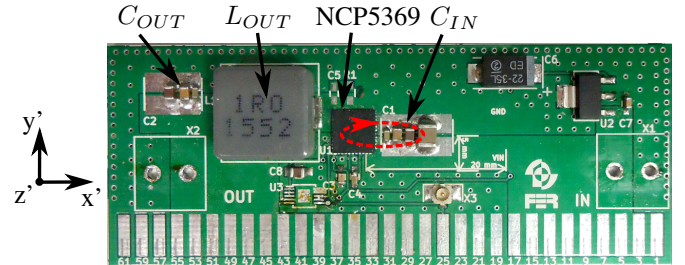


Fig. 3. Top view of the PCB. The red circle indicates the position of the radiating loop which is typically the dominant source of the radiated emissions of synchronous buck converters.

Re-arranging (5) and (6) allows to compute the index of the lowest overlapped harmonic n^{low} and that of the highest overlapped harmonic n^{up} for a given n , Δf and f_{sw} :

$$n^{low} = \left\lceil n \cdot \frac{f_{sw} - \Delta f}{f_{sw} + \Delta f} \right\rceil, \quad (7)$$

$$n^{up} = \left\lfloor n \cdot \frac{f_{sw} + \Delta f}{f_{sw} - \Delta f} \right\rfloor. \quad (8)$$

III. SYNCHRONOUS BUCK CONVERTER

A. Designed Converter

The converter analyzed in this paper is a non-regulated synchronous buck converter, whose simplified schematic is shown in Fig. 2. It is based on a NCP5369 controller which integrates a low-side (LS) field effect transistor (FET), a high-side (HS) FET, a digital control circuitry and a driving circuitry in one 40-pin package. The pulse width modulation (PWM) control signal is generated by an external generator applied to the corresponding input pin of the NCP5369.

The converter is implemented on a 1.55-mm thick 2-layer printed circuit board (PCB). All components are placed on the top layer. The bottom layer is a solid ground plane. The input decoupling network consists of four (1 μ F, 10 μ F, 22 μ F and 100 μ F) multilayer ceramic capacitors (MLCCs). The output filter consists of one 1- μ H inductor and three MLCCs (1 μ F, 10 μ F, 22 μ F). The top view of the PCB is shown in Fig. 3.

The red circle in Fig. 3 indicates the position of a radiating loop which is typically the dominant source of the radiated emissions of synchronous buck converters [10], [14]. The radiating loop is a consequence of the resonance in the input decoupling network. The resonance occurs between the capacitance of the FET in the off-state and the parasitic inductance of the input decoupling network L_{IDN} [10], [14].

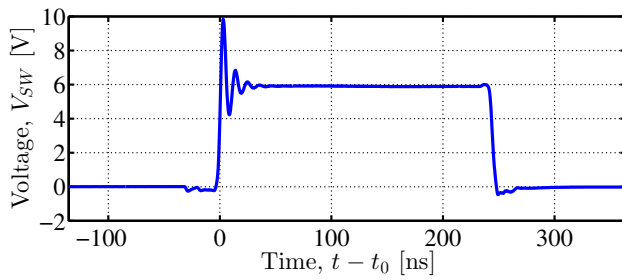


Fig. 4. Voltage of the switching node in the steady-state operation ($t_0 \gg 1/f_{sw}$). A resonance, which is typically the dominant source of the radiated emissions, can be seen at the rising edge.

The time-domain measurements are performed to validate the operation of the converter. The voltage of the switching node in the steady-state operation measured by a 300-MHz bandwidth oscilloscope is shown in Fig. 4. The efficiency of the converter is calculated from the measured data as:

$$\eta = \frac{V_{OUT} \cdot I_{OUT}}{V_{IN} \cdot I_{IN}}. \quad (9)$$

The SS technique is applied to the converter under the test conditions as follows. The input voltage V_{IN} is 6 V, the output voltage V_{OUT} is 1.8 V, the output current I_{OUT} of 3 A is set by the electronic load, while the switching frequency f_{sw} is 1.25 MHz. Under these conditions, the measured efficiency is 89.1%.

B. Calculation of the Radiated Emission

The analyzed converter is assumed to be an electrically small antenna. Its radiation characteristics are modeled by 5 collocated orthogonal dipole moments¹ which are extracted from the measurements performed exploiting the TEM cell and hybrid coupler [11], [12] and using the measurement setup shown in Fig. 5. The TEM cell is used as a near-field sensor of the generated fields, while the hybrid coupler is used to separate the contributions of the electric and magnetic dipole moments.

Positioning the converter in the TEM cell as shown in Fig. 5 allows to extract one electric and one magnetic dipole moment of the converter. The converter is rotated inside the TEM cell in three orthogonal dipole positions to extract the other dipole moments. The modular board system, which allows to position the converters inside the TEM cell in different positions, and the procedure for calculating the radiated fields from the extracted dipole moments are described in [11], [12].

C. Impact of the Spread-Spectrum Technique

The analysis of the impact of the SS technique on the radiated emissions of the converter is performed by applying the modulation to the control signal. The modulation function $f(f_m)$ is obtained through the same signal generator that produces the control signal. The parameters of the applied

¹More specifically, 3 magnetic and 2 electric dipole moments are used since the third electric dipole moment cannot be measured by the measurement setup because of the dimensions of the TEM cell and PCB.

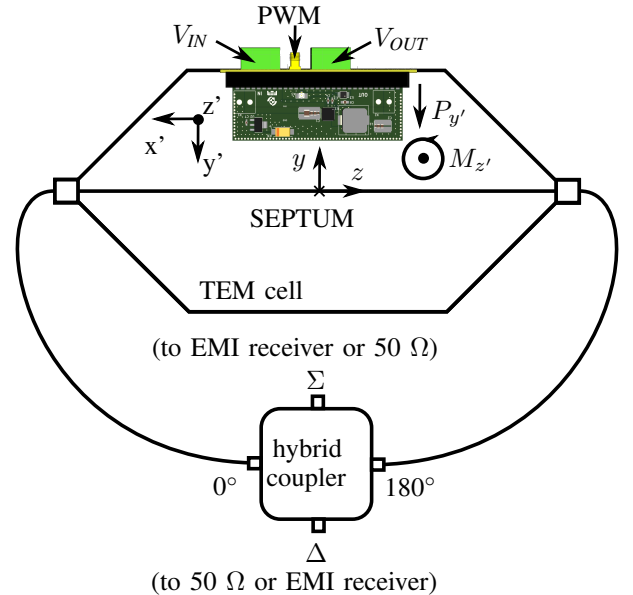


Fig. 5. Schematic representation of the measurement setup for the extraction of the dipole moments of the measured converter.

TABLE I
PARAMETERS OF THE APPLIED MODULATION.

Description	Parameter	Value
Modulation function	$f(f_m)$	triangular
Modulation index	m	1, 2, 5, 10, 20, 50, 100
Frequency deviation	Δf [kHz]	50, 100, 200

modulation are given in Table I. The parameters f_m and Δf are varied in the same range of values as in [7] and, for simplicity, only the triangular modulating function is considered here.

The measurements of the coupling to the TEM cell are performed by an EMI receiver with a peak detector. These measurements are used to calculate the radiated emissions of the converter at a distance of 10 m. The calculated radiated emissions before and after applying the SS technique are shown in Fig. 6. The emissions after applying the SS technique are shown for the parameters of the modulation which give the largest reduction ($\Delta f = 200$ kHz, $m = 50$). The maximum value of the radiated emissions before applying the SS technique is 13.8 dB $\mu\text{V}/\text{m}$ at 121.25 MHz, i.e. at the 97th harmonic. The impact of the SS technique is evaluated as the difference between the maximum value before and after applying the SS and reported in Fig. 7 for different modulation parameters.

The maximum reduction of the peak level of the first harmonic in [7] is approximately 7, 9 and 11 dB for Δf equal to 50, 100 and 200 kHz, respectively. The level of reduction increases with Δf . Here, the maximum reduction is approximately 6 dB for all three values of Δf .

In other words, although the equivalent modulation index is very large in these cases, the reduction is smaller than in [7] because of two reasons. The first one is the overlap of

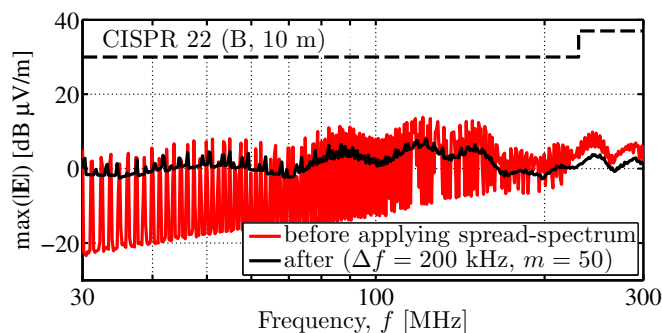


Fig. 6. Comparison of the spectrum before and after applying the SS technique.

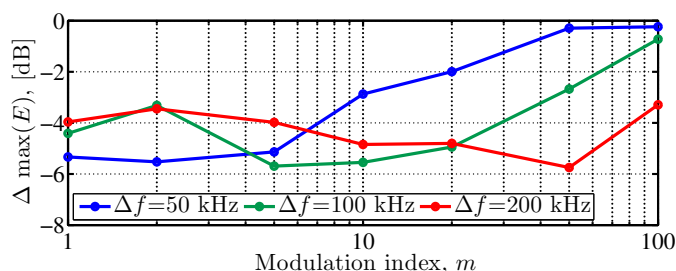


Fig. 7. Impact for different parameters of the modulation evaluated as the difference of the maximum value before and after applying the SS technique.

the spreading bandwidth of the higher-order harmonics, which limits the effectiveness of the SS technique. The indexes of the lowest and highest harmonics whose spreading bandwidth is overlapping with the one of the 97th harmonic for Δf of 50, 100 and 200 kHz calculated by (7) and (8) are given in Table II. The second reason is a different resolution bandwidth (RBW) used for the measurements of conducted and radiated emissions. The RBW is equal to 9 kHz for the conducted, while it is equal to 120 kHz for the radiated emissions [3]. As well known, RBW defines the separation of two harmonics which can be resolved by the EMI receiver, and, consequently, it determines how effective the SS can potentially be. A smaller RBW means that more spectral components can be used to spread the energy of the harmonic. Considering the values of the RBW, the SS technique is therefore potentially more effective in reducing the conducted than in reducing the radiated emissions.

Despite this and despite the fact that 63 harmonics are overlapped (for $\Delta f = 200$ kHz), the SS technique reduces the

TABLE II
 INDEXES OF THE HARMONICS WHOSE SPREADING BANDWIDTH
 OVERLAPS WITH THE ONE FOR $n = 97$.

Δf [kHz]	Δf_n [kHz]	n^{low}	n^{up}	# of overlapped spreading bandwidths calculated as $n^{up} - n^{low} + 1$
50	4850	90	105	16
100	9700	83	113	31
200	19400	71	133	63

radiated emission of the designed synchronous buck converter by up to 5.7 dB.

IV. CONCLUSION

The impact of the SS technique on the radiated emissions of a synchronous buck converter is analyzed. The converter operates at the switching frequency of 1.25 MHz. The maximum value of the radiated emissions occurs at 121.25 MHz, which is the 97th harmonic. For the frequency deviation of 200 kHz, the 97th harmonic is overlapped with 62 adjacent harmonics. This limits the effectiveness of the SS technique in reducing the radiated emissions. Despite the overlap, the reduction of up to 5.7 dB is obtained.

ACKNOWLEDGMENT

This work was supported in part by the Croatian Science Foundation (HRZZ) within the project "Advanced design methodology for switching dc-dc converters".

REFERENCES

- [1] F. L. Luo and H. Ye, "Investigation of EMI, EMS and EMC in power DC/DC converters," in *Proc. IEEE Int. Conf. on Power Electron. and Drive Systems (PEDS)*, vol. 1, Nov. 2003, pp. 572–577.
- [2] Z. Li and D. Pommerenke, "EMI specifics of synchronous DC-DC buck converters," in *Proc. IEEE Int. Symp. Electromagn. Compat.*, vol. 3, 2005, pp. 711–714.
- [3] C. Paul, *Introduction to Electromagnetic Compatibility*. Wiley, 2006.
- [4] V. Subotskaya, K. Cherniak, K. Hoermaier, and B. Deutschmann, "Emission reduction with spread spectrum clocking for switched capacitor buck converter," in *IEEE Int. Symp. Electromagn. Compat. and IEEE Asia-Pacific Symp. Electromagn. Compat. (EMC/APEMC)*, May 2018, pp. 297–302.
- [5] B. Auinger, B. Deutschmann, and G. Winkler, "Elimination of electromagnetic interference in communication channels by using spread spectrum techniques," in *Int. Symp. Electromagn. Compat. (EMC EUROPE)*, Sept. 2017, pp. 1–6.
- [6] B. Deutschmann, G. Winkler, and T. Karaca, "Emission reduction in Class D audio amplifiers by optimizing spread spectrum modulation," in *Int. Workshop Electromagn. Compat. of Integrated Circuits (EMC Compo)*, Nov. 2015, pp. 1–6.
- [7] F. Pareschi, R. Rovatti, and G. Setti, "EMI Reduction via Spread Spectrum in DC/DC Converters: State of the Art, Optimization, and Tradeoffs," *IEEE Access*, vol. 3, pp. 2857–2874, 2015.
- [8] F. Pareschi, G. Setti, R. Rovatti, and G. Frattini, "Practical Optimization of EMI Reduction in Spread Spectrum Clock Generators With Application to Switching DC/DC Converters," *IEEE Trans. Power Electron.*, vol. 29, no. 9, pp. 4646–4657, Sept. 2014.
- [9] F. Pareschi, G. Setti, and R. Rovatti, "A 3-GHz Serial ATA Spread-Spectrum Clock Generator Employing a Chaotic PAM Modulation," *IEEE Trans. Circuits Syst. I: Reg. Papers*, vol. 57, no. 10, pp. 2577–2587, Oct. 2010.
- [10] A. Bhargava, D. Pommerenke, K. Kam, F. Centola, and C. W. Lam, "DC-DC Buck Converter EMI Reduction Using PCB Layout Modification," *IEEE Trans. Electromagn. Compat.*, vol. 53, no. 3, pp. 806–813, Aug. 2011.
- [11] R. Blecic, H. Stimac, R. Gillon, B. Nauwelaers, and A. Baric, "Improved estimation of radiated fields of unintentional radiators by correction of the impedance mismatch between a transverse electromagnetic cell and a hybrid coupler," *IEEE Trans. Electromagn. Compat.*, vol. 60, no. 6, pp. 1717–1725, Dec. 2018.
- [12] R. Blecic, R. Gillon, B. Nauwelaers, and A. Baric, "EMC-Oriented Design of Output Stage of Synchronous Buck Converter," in *IEEE Int. Workshop Electromagn. Compat. of Integrated Circuits (EMC Compo)*, July 2017.
- [13] H. Black, *Modulation theory*. Van Nostrand, 1953.
- [14] K. Kam, D. Pommerenke, F. Centola, C. wei Lam, and R. Steinfeld, "EMC guideline for synchronous buck converter design," in *Proc. IEEE Int. Symp. Electromagn. Compat.*, Aug. 2009, pp. 47–52.